Charge fluctuations and correlation lengths in finite electrolytes

Young C. Kim* and Michael E. Fisher†
Institute for Physical Science and Technology, University of Maryland, College Park, Maryland 20742, USA
(Received 28 January 2008; published 23 May 2008)

Fluctuations of the charge Q_Λ inside a subdomain Λ embedded in an electrolyte contained in a finite cubical box of dimensions $L\times L\times L$ with periodic boundary conditions are investigated. When Λ is an $L\times L$ "slab" of width W, asymptotically exact expressions for the mean-square fluctuation $\langle Q_\Lambda^2\rangle$ are obtained in terms of the Lebowitz length $\xi_L(T,\rho)$ and of the "true" or asymptotic screening/decay length $\xi_{Z,\infty}(T,\rho)$ together, when the charge correlation decay is oscillatory, with the characteristic wavelength $\lambda_Z(T,\rho)$. In finite systems, the normalized charge fluctuations exhibit threefold scaling behavior in the ratios $\xi_{Z,\infty}/W$, W/λ_Z, and W/L. This enables one to estimate all the correlation lengths away from criticality quite precisely from finite-size grand canonical Monte Carlo simulations. The results for $\xi_{Z,\infty}$, λ_Z, and ξ_L are presented for the restricted primitive model or hard-sphere 1:1 electrolyte for densities $\rho\lesssim 1.3\rho_c$ and $T\gtrsim 4T_c$. The fitted values compare favorably with the expectations of generalized Debye-Hückel theory [Lee and Fisher, Europhys. Lett. **39**, 611 (1997)]; specifically, if $\xi_D\propto(T/\rho)^{1/2}$ is the Debye length, we find $\xi_{Z,\infty}<\xi_D<\xi_L$, although, since ion-pairing is neglected, the charge oscillations set in only for densities ~ 1.9 times larger than predicted.

DOI: 10.1103/PhysRevE.77.051502 PACS number(s): 64.70.F−, 64.60.F−, 05.70.Jk

I. INTRODUCTION

The behavior of charge fluctuations and correlations in an electrolyte has been a challenging problem for decades [1] and remains so both for theory and simulation. Here we focus on what may be learned from Monte Carlo simulations, particularly for various *correlation lengths*, by the careful study of finite-size effects. Specifically, a straightforward method is presented which, outside the critical region, enables charge-charge correlation lengths to be extracted precisely from finite-size Monte Carlo simulation data. Of course, the charge-charge correlation function $G_{ZZ}(\boldsymbol{r};T,\rho)$ for a classical fluid of overall ionic density ρ is well known to decay exponentially on the scale of the "true" or asymptotic screening length $\xi_{Z,\infty}(T,\rho)$, that is,

$$|G_{ZZ}(\boldsymbol{r};T,\rho)| \sim e^{-|\boldsymbol{r}|/\xi_{Z,\infty}} \quad \text{as } |\boldsymbol{r}|\to\infty . \tag{1}$$

According to simple Debye-Hückel (DH) theory [2], $\xi_{Z,\infty}(T,\rho)$ is identical to the Debye length $\xi_D(T,\rho)$, which, for ions carrying charges $q_\sigma=z_\sigma q$, is given by

$$1/\xi_D^2=\kappa_D^2=4\pi\bar{z}_2^2q^2\rho/Dk_BT, \tag{2}$$

where z_σ is the valence of ions of species σ while q is the elementary charge and $\rho=\Sigma_\sigma\rho_\sigma$ is the number density of ions (where ρ_σ represents the number density for species σ); further, $\bar{z}_2^2=\Sigma_\sigma z_\sigma^2\rho_\sigma/\rho$ is the mean square valence and D is the dielectric constant of the medium. However, DH theory is exact only when ρ approaches zero or T becomes large [3]. For finite $\rho>0$ and $T<\infty$, the decay length $\xi_{Z,\infty}(T,\rho)$ deviates from $\xi_D(T,\rho)$. But how large are these deviations for densities and temperatures on the scale of the critical values ρ_c and T_c? Furthermore, at higher densities the charge-charge correlation functions decay in oscillatory fashion with a characteristic wavelength, say $\lambda_Z(T,\rho)$ [4–7], which DH theory fails entirely to predict.

To understand better the various correlation lengths for ionic fluids, Lee and Fisher extended the original DH theory to nonuniform systems [6,7]. The resulting *generalized Debye-Hückel* (GDH) theory is the simplest theory among many others such as, e.g., those described in Refs. [8–13]. It actually provides a simple explicit expression for $\xi_{Z,\infty}(T,\rho)$ in the case of the restricted primitive model (RPM)—the basic two-component, $z_\sigma=\pm 1$, fluid of equisized hard spheres of diameter a, on which we will focus here. It transpires, furthermore, that the formula for $\xi_{Z,\infty}$ exhibits a bifurcation at $\kappa_Da\simeq 1.178$ beyond which, as originally suggested by Kirkwood [4], charge-charge oscillations with a wavelength $\lambda_Z(T,\rho)$ are predicted. When $\kappa_D\propto(\rho/T)^{1/2}$ increases, $\xi_{Z,\infty}(T,\rho)$ *decreases* and is predicted to remain always smaller than $\xi_D(T,\rho)$ up to the onset of the charge oscillations. In the oscillatory region the charge correlation length $\xi_{Z,\infty}$ *increases* and, according to GDH theory, diverges to infinity at a "point of crystallization." Since GDH theory is of mean-field character one would expect it to describe the behavior of charge (and density) correlations at least semiquantitatively at low densities and high temperatures. On approaching the vapor-liquid critical point, where density fluctuations dominate, GDH theory predicts, for *charge-symmetric* systems like the RPM, that $\xi_{Z,\infty}(T,\rho)$ *remains finite* at criticality [while the density correlation length $\xi_{N,\infty}(T,\rho)$ *diverges*]. This feature matches the exact solution of the $(d>2)$-dimensional ionic spherical models [14]. However, the validity of the finiteness prediction for the RPM and more realistic models remains to be verified; and a recent study suggests that it may actually fail [15]. But in the present work we consider only regions away from criticality.

The exact low-density expansions [3] show that $\xi_{Z,\infty}(T,\rho)$ deviates from $\xi_D(T,\rho)$ via a leading correction term varying as $\rho\ln\rho$ (which cannot be generated by GDH theory). However, recent simulations [16] for the RPM evaluated the Lebowitz length $\xi_L(T,\rho)$—see below—and found that these

*Present address: Laboratory of Chemical Physics, National Institute of Diabetes and Digestive and Kidney Diseases, National Institutes of Health, Bethesda, Maryland 20892, USA.
†Corresponding author. xpectnil@umd.edu

 ©2008 The American Physical Society

low-density expansions suffer from remarkably slow convergence. Indeed, even for densities $\rho^* = \rho a^3 \gtrsim 0.01$ and $T \simeq 10T_c$ the low-density expansion truncated after the leading correction term deviates significantly from the simulation estimates. Note, however, that this previous study [16] did not at all address the charge screening length $\xi_{Z,\infty}$. Initially, in fact, $\xi_{Z,\infty}$ seemed beyond computational reach; but our aim here is to extend the previous study and to demonstrate that, indeed, $\xi_{Z,\infty}(T,\rho)$ can be reliably estimated via simulation.

Following the definition (1) a "traditional" approach to calculating $\xi_{Z,\infty}(T,\rho)$ has been to use direct simulations of $G_{ZZ}(\boldsymbol{r};T,\rho)$ by fitting the long-distance behavior to a simple exponential. Simulating $G_{ZZ}(\boldsymbol{r};T,\rho)$, however, is computationally expensive and also lacks precision, since one needs the distribution at many distances. And, most significantly, finite-size effects on $G_{ZZ}(\boldsymbol{r};T,\rho)$ must be understood well before attempting to extract $\xi_{Z,\infty}$ with any reliability from the necessarily truncated data.

In this paper we present a straightforward method for extracting $\xi_{Z,\infty}(T,\rho)$ and other correlation lengths precisely from finite-size simulation data away from the critical point. When criticality is approached, however, the diverging density correlation length and large fluctuations inevitably hamper the reliable extraction of $\xi_{Z,\infty}(T,\rho)$ from simulations.

To compute $\xi_{Z,\infty}(T,\rho)$ we turn to an interesting aspect of the screening of the long-range Coulomb interactions, namely, the so-called "area law" of charge fluctuations. To be specific, consider a regular subdomain Λ with surface area A_Λ and volume $|\Lambda|$, embedded in a larger domain. If Q_Λ is the total fluctuating charge inside Λ, electroneutrality implies a vanishing mean value, $\langle Q_\Lambda \rangle = 0$. The mean square fluctuation $\langle Q_\Lambda^2 \rangle$, however, does not vanish but, rather, grows when $|\Lambda|$ increases. In the *absence* of screening, one expects $\langle Q_\Lambda^2 \rangle \sim |\Lambda|$; however, in a fully screened, bulk conducting fluid it transpires that $\langle Q_\Lambda^2 \rangle$ increases asymptotically only as the surface area A_Λ. This was first observed by van Beijeren and Felderhof [17] and later proven rigorously by Martin and Yalcin [18]. Following the interpretation of Lebowitz [19] one may then define a screening distance, $\xi_{\mathrm{L}}(T,\rho)$, via

$$\langle Q_\Lambda^2 \rangle / A_\Lambda \approx c_d \rho \bar{z}_2^2 q^2 \xi_{\mathrm{L}}(T,\rho) \quad \text{as } |\Lambda| \to \infty . \tag{3}$$

This measure has been called the Lebowitz length [3(a),6]; by selecting the numerical constant c_d one can normalize ξ_{L} to ξ_{D} when $\rho \to 0$: this yields $c_3 = \frac{1}{2}$. (Note that for the RPM one has $\bar{z}_2^2 = 1$.) As mentioned, the Lebowitz length has been studied via Monte Carlo simulations [16,20] in which it was extracted directly from observations of $\langle Q_\Lambda^2 \rangle$ for various subdomains Λ. Comparison with GDH theory and the low-density expansions [3] showed that the simulation estimates were consistent with the exact expansions for very low densities only up to $\rho a^3 \lesssim 0.005$ even at $T \gtrsim 10T_c$, while at densities up to $\rho a^3 \simeq 0.1$ they followed GDH theory semiquantitatively. But we will now demonstrate that the other correlation lengths, $\xi_{Z,\infty}(T,\rho)$ and $\lambda_Z(T,\rho)$, can also be extracted from essentially the same simulation data for $\langle Q_\Lambda^2 \rangle$ by paying closer attention to the effects of the finite dimensions of both the simulation boxes and the subdomains sampled.

To see this briefly, note that $\langle Q_\Lambda^2 \rangle$ can be obtained by integrating the charge-charge correlation function $G_{ZZ}(\boldsymbol{r};T,\rho)$ over the subdomain Λ of interest. Since $G_{ZZ}(\boldsymbol{r})$ at long distances (but much less than the box size) is described by an exponential decay controlled by the screening length $\xi_{Z,\infty}(T,\rho)$, it is understandable that $\langle Q_\Lambda^2 \rangle$ might be directly sensitive to $\xi_{Z,\infty}$; see Sec. II. Thus if one knows explicitly the relationship between $\langle Q_\Lambda^2 \rangle$ and $\xi_{Z,\infty}$ for a subdomain Λ, one can, at least in principle, extract $\xi_{Z,\infty}$ from a set of simulation data for $\langle Q_\Lambda^2 \rangle$ that, for each value of (T,ρ), encompasses a sufficiently broad range of domain sizes and box dimensions. Note that the same principle applies to estimating the wavelength $\lambda_Z(T,\rho)$.

The paper is organized as follows. A brief theoretical background regarding charge fluctuations in finite systems is presented in Sec. II. The fluctuations for spheres in a bulk system and slabs embedded in finite cubes with periodic boundary conditions are derived analytically. The asymptotically exact, analytical results are verified by simulations in Sec. III; the correlation lengths $\xi_{Z,\infty}$, λ_Z, and ξ_{L} are estimated from the simulation data and presented in Figs. 2–5. Section IV summarizes the conclusions.

II. THEORETICAL BACKGROUND

In this section we derive a formula for $\langle Q_\Lambda^2 \rangle$ for a slab in a three-dimensional $L \times L \times L$ simulation box with periodic boundary conditions. To that end, we first provide a brief analysis of the charge fluctuations in subdomains embedded in *bulk* systems $(L \to \infty)$ as developed by van Beijeren and Felderhof [17]. For simplicity, however, we present the theory only in a weak-coupling $(T \to \infty)$ or Debye-Hückel (DH) limit where the charge correlation function decays as $G_{ZZ}(r) \sim \exp(-\kappa_{\mathrm{D}} r)/r$. We then argue that the results can be applied to situations beyond the DH limit by replacing the inverse Debye screening length κ_{D} by the exact asymptotic screening length $\kappa = 1/\xi_{Z,\infty}$.

A. Charge fluctuations in finite subdomains

The charge fluctuation $\langle Q_\Lambda^2 \rangle$ is related to the charge-charge correlation function $G_{ZZ}(\boldsymbol{r};T,\rho)$ via

$$\langle Q_\Lambda^2 \rangle = \int_\Lambda \int_\Lambda d\boldsymbol{r} d\boldsymbol{r}' G_{ZZ}(\boldsymbol{r} - \boldsymbol{r}'), \tag{4}$$

where the integrations are performed over the subdomain Λ. We note that the Lebowitz length $\xi_{\mathrm{L}}(T,\rho)$ in Eq. (3) is defined asymptotically for $|\Lambda| \to \infty$; but one may define a finite-size Lebowitz length $\xi_\Lambda(T,\rho)$ for any finite Λ, via

$$\xi_\Lambda(T,\rho) \equiv \langle Q_\Lambda^2 \rangle / c_d \rho \bar{z}_2^2 q^2 A_\Lambda . \tag{5}$$

This approaches the bulk Lebowitz length $\xi_{\mathrm{L}}(T,\rho)$ when the subdomain Λ grows indefinitely in an infinite domain. If one assumes that $G_{ZZ}(\boldsymbol{r})$ then varies as $\exp(-r/\xi_{Z,\infty})$, with $r = |\boldsymbol{r}|$, which is true for $r \gg a$, it is reasonable for Λ much larger than the ionic size to assert that

$$\xi_\Lambda(T,\rho) \approx \xi_L(T,\rho)\mathcal{F}_\Lambda(\xi_{Z,\infty}/L_\Lambda) \quad \text{when } L_\Lambda \to \infty, \tag{6}$$

where L_Λ is a characteristic linear dimension of Λ (e.g., $L_\Lambda = |\Lambda|^{1/d}$), while $\mathcal{F}_\Lambda(x)$ is a scaling function which depends on the specific geometrical shape of Λ.

The behavior of $\mathcal{F}_\Lambda(x)$ for large and small $x=\xi_{Z,\infty}/L_\Lambda$ is easily determined: when $L_\Lambda \to \infty$ at fixed (T,ρ) one has $\xi_\Lambda(T,\rho) \to \xi_L(T,\rho)$. On the other hand, if $\xi_{Z,\infty} \gg L_\Lambda$ the screening effects on $\langle Q_\Lambda^2 \rangle$ will be truncated so that $\langle Q_\Lambda^2 \rangle$ will grow like the volume of Λ. Thus we conclude

$$\mathcal{F}_\Lambda(0) = 1 \quad \text{and} \quad \mathcal{F}_\Lambda(x) \sim 1/x \quad \text{as } x \to \infty. \tag{7}$$

When $G_{ZZ}(\boldsymbol{r};T,\rho)$ exhibits oscillatory behavior an additional multiplicative factor, $\cos(2\pi r/\lambda_Z + \theta)$, enters the asymptotic behavior: then it is natural to extend Eq. (6) to assert

$$\xi_\Lambda(T,\rho) \approx \xi_L(T,\rho)\tilde{\mathcal{F}}_\Lambda(\xi_{Z,\infty}/L_\Lambda, L_\Lambda/\lambda_Z). \tag{8}$$

Clearly one must have $\tilde{\mathcal{F}}_\Lambda(x,0) = \mathcal{F}_\Lambda(x)$ to describe the absence of charge oscillations in the limit $\lambda_Z \to \infty$.

Now one must recall that computer simulations are inevitably performed in a finite domain; specifically, we will address only periodic cubical boxes of side L. It is imperative that the resulting further finite-size effects on $\langle Q_\Lambda^2 \rangle$ be considered; but to accommodate the additional length scale L, it is natural to advance the threefold scaling ansatz

$$\xi_\Lambda(L;T,\rho) \approx \xi_L(T,\rho)\mathcal{G}_\Lambda\left(\frac{L_\Lambda}{L}; \frac{\xi_{Z,\infty}}{L_\Lambda}, \frac{L_\Lambda}{\lambda_Z}\right). \tag{9}$$

To describe the threefold limits $L \to \infty$, $L_\Lambda \to \infty$, $\lambda_Z \to \infty$, one needs $\mathcal{G}_\Lambda(0;0,0) = 1$; but when $L \to \infty$ with $L_\Lambda < \infty$, the previous bulk results are recovered provided $\mathcal{G}_\Lambda(0;x,y) = \tilde{\mathcal{F}}_\Lambda(x,y)$. In the following subsections we compute these scaling functions explicitly in the DH limit for various special geometries and, in so doing, will verify the scaling expectations.

It is natural to inquire as to the domain of validity of the asymptotic scaling ansatz (9). Implicit is the assumption of a large subdomain Λ so that $L_\Lambda/a \gg 1$. From this (necessarily since $L_\Lambda \le L$) a large simulation box is imperative, i.e., $L/a \gg 1$ is needed. The dependence on $\xi_{Z,\infty}/L_\Lambda$, which we may suppose is of the same order as $\xi_{Z,\infty}/L$, is more subtle. In the general case of finite-size scaling this ratio may be large *or* small since, indeed, one expects finite-size scaling to be valid for $L/a \gg 1$ right up to and including criticality. (See, e.g., [16].) However, as mentioned, we will calculate the scaling function in Eq. (9) for the more limited regime in which exponential charge screening is valid. Then the character of the decay of the envelope of $G_{ZZ}(\boldsymbol{r})$ plays a more crucial role and one must anticipate that in the critical region, where the density correlation length $\xi_{N,\infty}$ diverges, the calculated form for $\mathcal{G}_\Lambda(x;y,z)$ will no longer be adequate.

Apart from this situation, further special considerations apply when the onset of charge oscillations is approached. As discussed further below, a second, albeit subdominant exponential decay length then appears. The associated correction terms affect the accuracy of the dominant scaling expression.

B. Debye-Hückel limit

The charge-charge correlation function can be written generally as

$$G_{ZZ}(\boldsymbol{r},\boldsymbol{r}') = \sum_\alpha q_\alpha^2 \rho_\alpha \delta(\boldsymbol{r}-\boldsymbol{r}') - \sum_\alpha \sum_\beta q_\alpha^2 \rho_\alpha q_\beta^2 \rho_\beta g(\boldsymbol{r},\boldsymbol{r}'), \tag{10}$$

where, in the DH regime with vanishing ionic size ($a \to 0$), $g(\boldsymbol{r},\boldsymbol{r}')$ satisfies the Debye-Hückel partial differential equation [2,6]

$$\nabla^2 g - \kappa^2 g = -(4\pi/Dk_BT)\delta(\boldsymbol{r}-\boldsymbol{r}'), \tag{11}$$

in which κ is the inverse screening length. In the full DH limit, one has $\kappa = \kappa_D = 1/\xi_D$ but the validity of Eq. (11) will extend to regimes in which one leading exponential decay, as in Eq. (1), dominates.

On using Eq. (10), the charge fluctuations in a subdomain Λ can be expressed as

$$\langle Q_\Lambda^2 \rangle = \int_\Lambda d\boldsymbol{r} \int_\Lambda d\boldsymbol{r}' G_{ZZ}(\boldsymbol{r},\boldsymbol{r}') = \sum_\alpha q_\alpha^2 \rho_\alpha |\Lambda| \left[1 - \sum_\alpha q_\alpha^2 \rho_\alpha \int_\Lambda d\boldsymbol{r}\phi(\boldsymbol{r}) \right], \tag{12}$$

where the Λ-averaged correlation function is

$$\phi(\boldsymbol{r}) \equiv \frac{1}{|\Lambda|}\int_\Lambda g(\boldsymbol{r},\boldsymbol{r}')d\boldsymbol{r}'. \tag{13}$$

It follows from Eq. (11) that $\phi(\boldsymbol{r})$ satisfies

$$\nabla^2\phi - \kappa^2\phi = -(4\pi/Dk_BT|\Lambda|)\Theta_\Lambda(\boldsymbol{r}), \tag{14}$$

where the characteristic function $\Theta_\Lambda(\boldsymbol{r}) = 1$ if $\boldsymbol{r}$ lies inside Λ but vanishes otherwise. Furthermore, $\phi(\boldsymbol{r})$ and its derivatives must be continuous everywhere including the boundary of Λ. By solving Eq. (14) with appropriate boundary conditions (including decay to zero as $|\boldsymbol{r}| \to \infty$) and integrating the solution over Λ, one can obtain the charge fluctuations via Eq. (12).

As the simplest example consider a sphere of radius R embedded in a bulk system. This case was originally studied by van Beijeren and Felderhof [17] and has been revisited more recently by Jancovici [21]. For a spherical geometry the solution of Eq. (14) for $r < R$ is

$$\phi(r) = \frac{3}{Dk_BT\kappa^2R^3}\left[1 - (1+\kappa R)\exp(-\kappa R)\frac{\sinh \kappa r}{\kappa r} \right]. \tag{15}$$

Integrating over the sphere and using Eq. (12) yields

$$\langle Q_\Lambda^2 \rangle = Dk_BT(1+\kappa R)\frac{e^{-\kappa R}}{\kappa}(\kappa R \cosh \kappa R - \sinh \kappa R). \tag{16}$$

The normalized finite-size Lebowitz length is then given by

$$\xi_\Lambda(R;T,\rho) = \frac{2}{\kappa^3 R^2}(1+\kappa R)e^{-\kappa R}(\kappa R\cosh\kappa R - \sinh\kappa R), \tag{17}$$

from which one finds $\xi_L(T,\rho)=1/\kappa=\xi_D$ in the DH limit as expected. Evidently scaling is obeyed with a scaling function, taking $x\equiv\xi_{Z,\infty}/R$, given explicitly by

$$\mathcal{F}_\Lambda(x) = 2(1+x)e^{-1/x}[\cosh(1/x) - x\sinh(1/x)]. \tag{18}$$

One readily checks that $\mathcal{F}_\Lambda(0)=1$, while $\mathcal{F}_\Lambda(x)\approx 2/3x$ when $x\to\infty$ so confirming Eq. (7).

Beyond the DH limit, the charge-charge correlation function decays exponentially with the asymptotic correlation length $\xi_{Z,\infty}$ rather than ξ_D. Furthermore, for a finite ionic diameter, $a>0$, the charge-charge correlation function deviates strongly from a simple exponential function near $r=a$. One may thus ask: "Can the expression (18) be applied to such cases specifically, for example, to the RPM?" In response, notice that when $R\gg a$, the integrations in Eqs. (12) and (13) are dominated by $\boldsymbol{r}$ near the surface $|\boldsymbol{r}|=R$. Furthermore, the nonexponential variation arising from the region near $|\boldsymbol{r}|=a$ should contribute mainly to the nonuniversal scaling amplitude $\xi_L(T,\rho)$ in Eq. (6). Hence in leading order one should expect the same universal scaling function $\mathcal{F}_\Lambda(x)$ for spherical domains but with a correction factor differing from unity by terms varying as $(a/R)^\psi$ with $\psi\geq 1$.

When charge oscillations arise, GDH theory indicates that at long distances $G_{ZZ}(r;T,\rho)$ behaves as $r^{-1}\exp(-r/\xi_{Z,\infty})\cos(2\pi r/\lambda_Z+\theta)\sim \mathrm{Re}[e^{-(\kappa_r+i\kappa_i)r+i\theta}]$ with $\kappa_r=1/\xi_{Z,\infty}$ and $\kappa_i=2\pi/\lambda_Z$, where θ is a phase shift and Re[·] denotes the real part. Hence by replacing κ in Eqs. (14)–(17) simply by a complex parameter $\kappa=\kappa_r+i\kappa_i$, and taking the real part, one can obtain the full scaling function $\tilde{\mathcal{F}}_\Lambda(\xi_{Z,\infty}/R, R/\lambda_Z)$ for a spherical subdomain in a bulk system. (Note that the phase shift θ plays no role in this step.)

For applications to simulations, however, one now needs to calculate $\langle Q_\Lambda^2\rangle$ for a sphere that is embedded in a finite cubical box with periodic boundary conditions. The task of solving the differential equation (14) for such a geometry is nontrivial, making spherical subdomains unattractive for simulations. Accordingly, we turn to a subdomain with a simpler geometry, namely, a "periodic slab" of width (or thickness) $W<L$.

C. Charge fluctuations in slabs

Figure 1(a) presents the geometry of a periodic slab of dimension $L\times L\times W$ embedded in a periodic cubical box of side L (as considered in our simulations). Owing to the periodic boundary conditions, the two coordinates parallel to the surface planes of the slab become irrelevant, and one can map the slab, of relative width $w=W/L$, onto a one-dimensional periodic interval of period L as shown in Fig. 1(b). The partial differential equation (14) then reduces to an ordinary differential equation, namely,

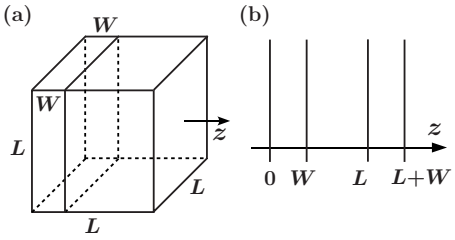

FIG. 1. (a) Schematic diagram of a "periodic slab" of width W inside a periodic cubical simulation box of side L and (b) corresponding one-dimensional projection onto the z axis.

$$\frac{d^2\phi(z)}{dz^2} - \kappa^2\phi(z) = -\frac{4\pi}{Dk_BTWL^2}\Theta_W(z), \tag{19}$$

where $\Theta_W(z)=1$ for $z\in(nL,nL+W)$, with $n=0,\pm1,\pm2,\ldots$, but $\Theta_W=0$ otherwise. With the boundary conditions that $\phi(z)$ and $(d\phi/dz)$ are continuous at $z=nL$ and $nL+W$ $(n=0,\pm1,\ldots)$ it is straightforward to obtain the solution for $0\leq z\leq W$, namely,

$$\phi(z) = \frac{4\pi}{Dk_BT\kappa^2WL^2}\left[1 + \frac{(e^{\kappa L}-e^{\kappa W})e^{-\kappa z}}{2(1-e^{\kappa L})} + \frac{(e^{-\kappa L}-e^{-\kappa W})e^{\kappa z}}{2(1-e^{-\kappa L})}\right]. \tag{20}$$

Integration then yields the scaling behavior

$$\xi_\Lambda(L)/\xi_L \approx \tilde{\mathcal{F}}(w;x) = \frac{1-e^{-1/x}+e^{-1/wx}-e^{-(1-w)/wx}}{1-e^{-1/wx}}, \tag{21}$$

with $x\equiv\xi_{Z,\infty}/W$ and $w=W/L$. In the thermodynamic limit $(w=0)$, one obtains $\mathcal{F}_\Lambda(x)=1-e^{-1/x}$ with $\mathcal{F}_\Lambda(0)=1$ and $\mathcal{F}_\Lambda(x)\approx 1/x$ when $x\to\infty$ in accord with the general expectations.

Finally, in the presence of asymptotic charge oscillations when $\lambda_Z<\infty$, the full scaling function, $\mathcal{G}_\Lambda$, appearing in Eq. (9) can be obtained, as explained, by replacing κ in Eq. (20) by $\kappa_r+i\kappa_i$ and taking the real part. After some algebra, one then finds, with, we recall, $w=W/L$, $x=\xi_{Z,\infty}/L$ and, now, $y\equiv 2\pi W/\lambda_Z$,

$$\mathcal{G}_\Lambda(w;x,y) = \mathcal{H}(w;x,y)/\mathcal{K}(w;x,y), \tag{22}$$

where the numerator and denominator are

$$\mathcal{H}(w;x,y) = 1 - e^{-2/wx} - [e^{-1/x} - e^{-(2-w)/wx}]\cos y + [e^{-(1+w)/wx} - e^{-(1-w)/wx}]\cos[(1-w)y/w], \tag{23}$$

$$\mathcal{K}(w;x,y) = 1 + e^{-2/wx} - 2e^{-1/wx}\cos(y/w). \tag{24}$$

This verifies the full scaling ansatz (9) and we may note that when $y=0$ (i.e., $\lambda_Z=\infty$), one recovers Eq. (21).

III. CORRELATION LENGTHS OF THE RPM

We have performed grand canonical Monte Carlo simulations for the RPM at $T^*=k_BTa/q^2=0.2\simeq 4T_c^*$ and $T^*=0.5$ for

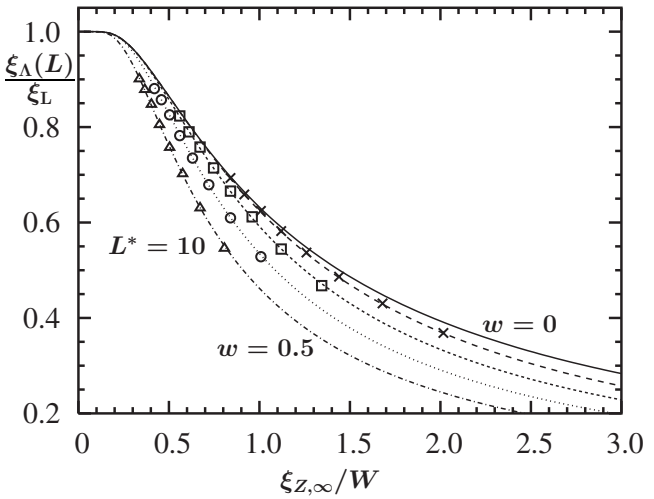

FIG. 2. The finite-size Lebowitz ratio $\xi_\Lambda(L;T,\rho)/\xi_L(T,\rho)$ fitted as a function of $\xi_{Z,\infty}(T,\rho)/W$ for, from the left, reduced slab widths $w=W/L=0.5$, 0.4 ,0.3, and 0.2. The symbols on each dotted curve represent simulation data for the RPM at $T^*=0.5$ and $\rho^*=0.0025$ with, successively from the lowest values of ξ_Λ/ξ_L, box sizes $L^*=L/a=10,12,\ldots,24$, while the various dotted curves are the fitted analytical expression (21) for the fixed values of w; the solid curve is the corresponding result for $L\to\infty$, i.e., $w\to 0$.

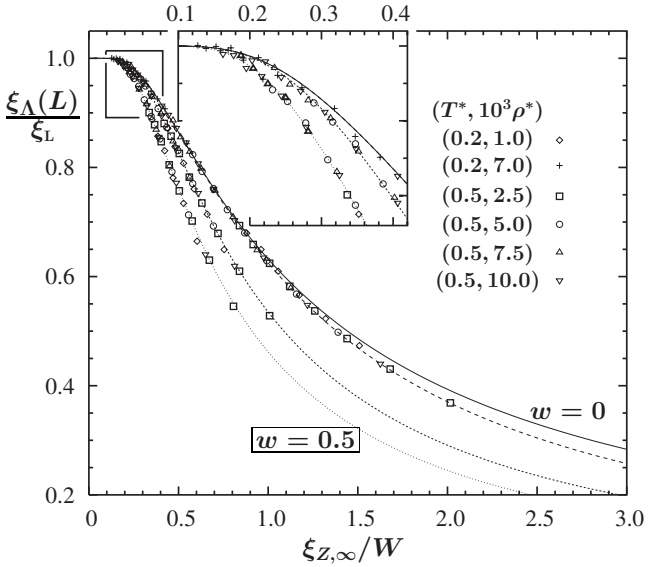

FIG. 3. Scaling plots for fixed relative slab widths w as in Fig. 2, showing the finite-size Lebowitz ratios $\xi_\Lambda(L)/\xi_L$ as a function of $\xi_{Z,\infty}/W$ (with $w=W/L=0.2$, 0.4, and 0.5) where, now, the different symbols represent data for densities from $\rho^*=0.001$ up to 0.01 for the previous range of box sizes and for $T^*=0.2$ and 0.5. As previously, the dotted curves depict the corresponding fitted expressions, while the limit $w\to 0$ $(L\to\infty)$ is shown solid. The framed region for $\xi_\Lambda/\xi_L\gtrsim 0.9$ is enlarged in the inset.

$0.001\le\rho^*\le 0.1$ employing box sizes $L^*=L/a$ varying from 10 to as large as 24 at low densities, $\rho^*\le 0.01$. In order to accelerate the computations, a finely discretized lattice version of the RPM has been adopted [22] using a $\zeta\equiv a/a_0=5$ level (where a_0 is the lattice spacing). Note, however, that it is well established that for $\zeta\gtrsim 3$ the fine-lattice discretization has no qualitative effect on the thermodynamic or finite-size properties [23]. For the $\zeta=5$ model one has $T_c^*\simeq 0.05069$ and $\rho_c^*\simeq 0.079$ [24,25].

At each state point (T^*,ρ^*), histograms of fluctuating charges Q_Λ for slabs with $w=W/L=0.2,0.3,0.4,0.5$ were collected; see Fig. 1. To enhance the information extracted from these data, a multihistogram reweighting technique was adopted [26]: the ensemble average of the charge fluctuations $\langle Q_\Lambda^2\rangle$ may then be computed for any desired T^* and ρ^* in the range encompassed by the state points simulated. The finite-box finite-size Lebowitz length $\xi_\Lambda(L;T,\rho)$ is calculated via Eq. (5) setting $A_\Lambda=2L^2$ for all slabs. Finally, to estimate $\xi_{Z,\infty}(T,\rho)$, $\lambda_Z(T,\rho)$, and $\xi_L(T,\rho)$, least-square fits of the simulation data for $\xi_\Lambda(L;T,\rho)$ to the general threefold scaling ansatz (9) were performed by using the theoretical expressions (22)–(24) with the three fitting parameters, x, y, and ξ_L.

At low densities ($\rho^*\lesssim 0.03$), the fits to Eqs. (22)–(24) yield y close to zero or $\lambda_Z(T,\rho)=\infty$, so that, as anticipated, the charge-charge correlation function appears to decay exponentially without oscillations. On the other hand, when $\rho^*>0.03$, better fits are obtained with $y>0$ thereby indicating the presence of charge oscillations. However, one may still ask for explicit evidence of the validity of the scaling behavior (9) with Eqs. (22)–(24) for the charge fluctuations under the conditions in which our simulations were performed.

To address this issue, we present in Fig. 2 plots of the finite-size ratio $\xi_\Lambda(L)/\xi_L$ vs $\xi_{Z,\infty}/W$ $(=x/w)$ at $T^*=0.5$ and $\rho^*=0.0025$ (corresponding to $X\equiv\kappa_D a\simeq 0.25$) using the fitted ξ_L and $\xi_{Z,\infty}$ values. The various dotted curves represent the analytical expression (21) for $w\equiv W/L=0.2,0.3,0.4,0.5$ while the solid curve is the analytical result for $w=0$ (i.e., $L=\infty$). The excellent collapse of the simulation data for system sizes L^*, ranging from 10 to 24 onto the theoretical plots parametrized by w, demonstrate that the scaling description of $\xi_\Lambda(L)$ remains valid even for L^* as low as 10 and confirms the validity of the fitting procedure. It is notable that the fitted value of $\xi_L(T,\rho)$ exceeds the largest simulated value $\xi_\Lambda(L;T,\rho)$ by 10%.

To confirm the scaling behavior of $\xi_\Lambda(L)$ also at higher densities, Fig. 3 presents simulation data at $T^*=0.5$ and also $T^*=0.2$ for various densities below $\rho^*=0.03$ (with $X=\kappa_D a$ ranging between 0.25 and 0.66) where no charge oscillations are indicated. Evidently the scaling behavior is remarkably well verified.

At higher densities, $\rho^*>0.03$, we found that optimal fitting of the simulation data to Eqs. (22)–(24) was obtained with $y>0$ or $\lambda_Z<\infty$. The scaling function for $\xi_\Lambda(L)$ then contains the extra variable, $y=2\pi W/\lambda_Z(T,\rho)$. Figure 4 illustrates the quality of fitting for $w=0.2$. Note that when $\lambda_Z=\infty$ (so that $y=0$), the plot (on the front face) matches that in Fig. 3. It was observed that the simulation data are well described by the scaling functions (22)–(24) for $X=\kappa_D a\gtrsim 2.0$.

The resulting correlation lengths, $\xi_{Z,\infty}$, λ_Z, and ξ_L, obtained from the fitting for $T^*=0.2\simeq 4T_c^*$ are plotted in Fig. 5 vs $X=a/\xi_D$, which increases as $\sqrt{\rho}$. Also included, as solid

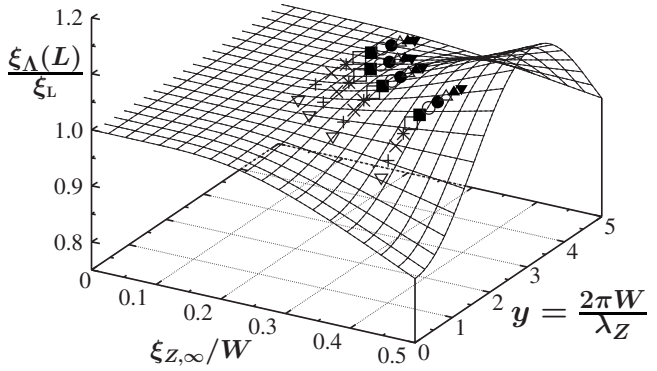

FIG. 4. Three-dimensional plot of the finite-size Lebowitz ratio $\xi_\Lambda(L)/\xi_L$ for $w=W/L=0.2$ and $L^*=10$, 12, 14, and 16, in terms of the two scaling variables $\xi_{Z,\infty}/W(=x/w)$ and $y=2\pi W/\lambda_Z$. The symbols derive via fitting to Eqs. (22)–(24) from data for $T^*=0.2$ and densities increasing (to the right) from $\rho^*=0.05$ in steps of $\Delta\rho^*=0.005$ up to $\rho^*=0.10$.

curves, are the predictions of GDH theory. Overall, the simulation results reflect rather well the trends exhibited by GDH theory. Several points are worthy of mention. First, the Lebowitz length obtained here—see the pluses in Fig. 5—is consistent with the previous results for $T^*=0.5$ [16]; specifically, $\xi_L(T,\rho)$ rises above the Debye length $\xi_D(T,\rho)$ by 10–30 % at higher densities while GDH theory overestimates $\xi_L(T,\rho)$ by only 5% or so above $\kappa_D a \simeq 1$.

Second, our simulations suggest the onset of oscillatory charge correlation decay at $X=\kappa_D a \gtrsim 1.4$ while GDH theory predicts a charge oscillation threshold at $\kappa_D a \simeq 1.178$ [5,3(a)]. At this value, sometimes labeled X_K in honor of Kirkwood [4], the GDH asymptotic correlation length exhibits a bifurcation point. Near X_K the correlation length falls

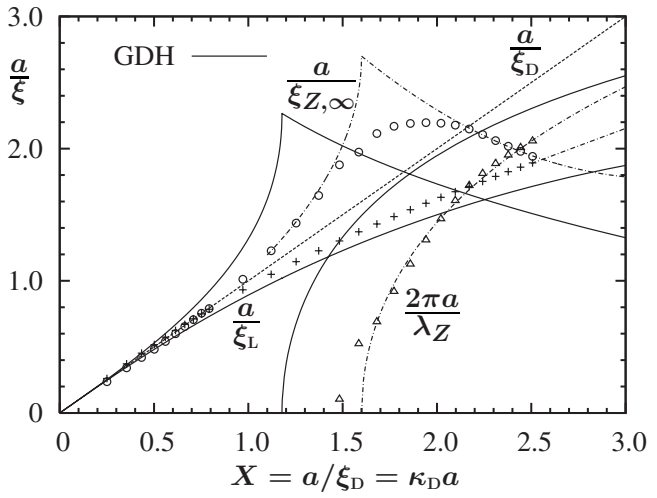

FIG. 5. The inverse correlation lengths $a/\xi_{Z,\infty}$, a/ξ_L, and $2\pi a/\lambda_Z$ for the RPM at $T^*=0.2$ and for densities up to $\rho^* \simeq 0.1$ plotted vs $X=a/\xi_D=\kappa_D a \propto \rho^{1/2}$ as derived from simulations using box sizes $L^*=L/a$ from 10 to 24. The diagonal dashed line merely represents a/ξ_D. The three solid curves portray the corresponding predictions of GDH theory while the two dotted-dashed curves for $a/\xi_{Z,\infty}$ and $2\pi a/\lambda_Z$ indicate, approximately, the likely correct behavior in the interval $1.3 \lesssim X \lesssim 2.2$.

rapidly in *square-root* fashion, namely, as

$$\xi_{Z,\infty}(T,\rho) - \xi_{Z,\infty}(T,\rho_K) \approx b_-(X_K - X)^{1/2}, \tag{25}$$

for $X \leq X_K$, i.e., when $\rho \to \rho_K(T)$ from below; above the Kirkwood threshold, however, it increases *linearly* as

$$\xi_{Z,\infty}(T,\rho) - \xi_{Z,\infty}(T,\rho_K) \approx b_+(X - X_K), \tag{26}$$

where both amplitudes b_- and b_+ are positive. At the same time, the oscillatory wave number $k_Z(T,\rho) \equiv 2\pi/\lambda_Z(T,\rho)$ increases sharply (above X_K) according to a square root law. This behavior is evident from the solid curves in Fig. 5 and is seen explicitly in the theoretical plots displayed in Fig. 1 of (both) Refs. [3(a)] and [6].

On the other hand our extrapolations of the simulation data for $\xi_{Z,\infty}$—see the open circles in Fig. 5—exhibit a corresponding asymmetric maximum vs X around $X=1.7$; but it is very smoothly rounded. The reduced wave number $k_Z a = 2\pi a/\lambda_Z$—see the open triangles in Fig. 5— does show a sharp onset; but the behavior above the threshold could well be interpreted as a *linear* rise with X rather than a square-root dependence. These differences, we believe, represent shortcomings of the present numerical analysis resulting primarily from the necessarily restricted box sizes that were computationally accessible.

Indeed, it seems most probable that the RPM (and other comparable models) will exhibit bifurcations obeying Eqs. (25) and (26) [and, similarly, for $k_Z(T,\rho)$]. In that case, when $\rho \to \rho_K(T)$ from below, a *second* but shorter charge correlation length, say $\xi^-_{Z,\infty}=1/\kappa^-$ appears, as again seen in Fig. 1 of Refs. [6,3(a)]. This derives from the subleading pole of the Fourier transform $\hat{G}_{ZZ}(\boldsymbol{k})$ which approaches the leading pole so that $\Delta\kappa=(\kappa^- - \kappa)$ decreases and vanishes when $\rho=\rho_K$. The main consequence is that for ρ close to ρ_K the charge-charge correlation function gains a relatively large correction, varying like $e^{-\Delta\kappa r}$, which is not accounted for by Eq. (11) or (19). Such an exponentially decaying correction to the scaling function (22) should become negligible for large enough box sizes L; but for restricted sizes the accuracy of fits near the Kirkwood point will be markedly reduced.

To make allowance for the expected behavior in Eqs. (25) and (26) and for the associated lower accuracy, we have indicated by the dotted-dashed curves in Fig. 5 what we feel is a more reasonable, albeit approximate, rendition of the variation of $\xi_{Z,\infty}(T,\rho)$ and $\lambda_Z(T,\rho)$ for the RPM in the range $X=\kappa_D a=1.3-2.2$. The Kirkwood threshold, as drawn in, is close to $X_K=1.63$; that corresponds to a density ~ 1.9 times larger than the GDH prediction. It must be emphasized, however, that this is no more than a rough guess: the "observed" threshold at $X_K \simeq 1.45$ would suggest a density factor of only ~ 1.5. Other approximate treatments, such as the generalized mean spherical model [10] which yields $X_K \simeq 1.228$, also seem to fall short by factors of 1.25–1.40 or greater.

To improve on our estimates for X_K, data for significantly larger system sizes would be needed. Such simulations would, we believe, reveal increasingly sharper maxima in the fits for $\xi_{Z,\infty}(T,\rho)$ better approximating Eqs. (25) and (26). Correspondingly, a steeper vanishing of the wave number $k_Z(T,\rho)$ should appear. It may also be, however, that more precise simulation data for a larger range of slab widths

could be of assistance in sharpening the fitted bifurcation.

It should be remarked, however, that the relatively larger value of the Kirkwood threshold, especially at low temperatures, is to be expected in light of the known importance of Bjerrum ion pairing which, in essence, serves to reduce the density of free ions and, hence, leads to a renormalization of the GDH values [6,7,27,28]. The same will apply to other approximations (e.g., [10]) that neglect pairing.

Finally, although the expected singular variation of $\xi_{Z,\infty}(T,\rho)$ cannot be fully captured, we believe that outside the rounding region (say, $X=1.75\pm0.25$) the values obtained for $\xi_{Z,\infty}(T,\rho)$ and $\lambda_Z(T,\rho)$ are reliable and reasonably accurate. At the same time it is worth commenting that the estimates for the Lebowitz length $\xi_L(T,\rho)$ are remarkably *insensitive* to the bifurcation and appearance of oscillatory decay.

IV. CONCLUSIONS

In summary, we have presented a surprisingly straightforward and simple method for estimating the asymptotic charge screening length $\xi_{Z,\infty}(T,\rho)$, the oscillation wavelength $\lambda_Z(T,\rho)$, and the Lebowitz length $\xi_L(T,\rho)$ of an electrolyte from simulations of the charge fluctuations inside slabs of a range of widths W. An asymptotically exact formula for the mean-square charge fluctuation $\langle Q_\Lambda^2\rangle$ has been derived for slabs contained in a periodic cubical box of side L. The normalized finite-size charge fluctuations then exhibit threefold scaling behavior in terms of the variables W/L, $\xi_{Z,\infty}/W$, and W/λ_Z. By fitting simulation data to the exact scaling form we were able to extract all the correlation lengths precisely. The results are in good semiquantitative agreement with the predictions of GDH theory. Furthermore, the fits reveal the onset of oscillatory charge decay at higher densities; however, the expected singular variation of $\xi_{Z,\infty}$ and λ_Z is not revealed in the numerics. Nevertheless, the threshold density for oscillations is clearly higher than predicted by the GDH and other approximate theories. Finally, although the area law underlying the definition of ξ_L is not available for *uncharged* fluid systems, the investigation of density and composition fluctuations within suitable subdomains may still prove useful in studying the decay of correlations in neutral fluids via simulations.

[1] See, e.g., J.-P. Hansen and I. R. McDonald, *Theory of Simple Liquids*, 2nd ed. (Academic, London, 1986), Chap. 10; and M. E. Fisher, J. Stat. Phys. **75**, 1 (1994); G. Stell, *ibid.* **78**, 197 (1994).

[2] For a systematic modern account, see D. A. McQuarrie, *Statistical Mechanics* (Harper-Collins, New York, 1976), Chap. 15.

[3] For the deviations from DH theory at low density and high T, see (a) S. Bekiranov and M. E. Fisher, Phys. Rev. Lett. **81**, 5836 (1998); (b) Phys. Rev. E **59**, 492 (1999); (c) M. E. Fisher and S. Bekiranov, Physica A **263**, 466 (1999).

[4] J. G. Kirkwood, Chem. Rev. (Washington, D.C.) **19**, 275 (1936).

[5] F. H. Stillinger and R. Lovett, J. Chem. Phys. **48**, 3858 (1968).

[6] B. P. Lee and M. E. Fisher, Europhys. Lett. **39**, 611 (1997).

[7] B. P. Lee and M. E. Fisher, Phys. Rev. Lett. **76**, 2906 (1996).

[8] J. S. Høye, J. L. Lebowitz, and G. Stell, J. Chem. Phys. **61**, 3253 (1974).

[9] C. W. Outhwaite, *Statistical Mechanics. A Specialist Periodic Report*, edited by K. Singer (The Chemical Society, London, 1975), Vol. 2.

[10] R. J. H. Leote de Carvalho and R. Evans, Mol. Phys. **83**, 619 (1994).

[11] G. Stell, J. Stat. Phys. **78**, 197 (1995); *New Approaches to Problems in Liquid-State Theory*, edited by C. Caccamo, J.-P. Hansen, and G. Stell (Kluwer Academic, Dordrecht, 1999).

[12] D. M. Zuckerman, M. E. Fisher, and B. P. Lee, Phys. Rev. E **56**, 6569 (1997).

[13] A. Ciach, W. T. Góźdź, and R. Evans, J. Chem. Phys. **118**, 3702 (2003).

[14] J.-N. Aqua and M. E. Fisher, Phys. Rev. Lett. **92**, 135702 (2004); J. Phys. A **37**, L241 (2004).

[15] S. K. Das, Y. C. Kim, and M. E. Fisher reported by M. E. Fisher at the CECAM Workshop on Fluid Phase Behavior, 2007, ENS, Lyon, and at STATPHYS 23 in Genoa, 2007, accessible at ⟨http://www.cecam.org/workshop-4-157.html?presentation_id=2070⟩.

[16] Y. C. Kim, E. Luijten, and M. E. Fisher, Phys. Rev. Lett. **95**, 145701 (2005).

[17] H. van Beijeren and B. U. Felderhof, Mol. Phys. **38**, 1179 (1979).

[18] Ph. A. Martin and T. Yalcin, J. Stat. Phys. **22**, 435 (1980).

[19] J. L. Lebowitz, Phys. Rev. A **27**, 1491 (1983).

[20] The earliest simulations were for a two-dimensional system by D. Levesque, J.-J. Weis, and J. L. Lebowitz, J. Stat. Phys. **100**, 209 (2000).

[21] B. Jancovici, J. Stat. Phys. **110**, 879 (2003).

[22] A. Z. Panagiotopoulos, J. Chem. Phys. **112**, 7132 (2000).

[23] Y. C. Kim and M. E. Fisher, Phys. Rev. Lett. **92**, 185703 (2004); S. Moghaddam, Y. C. Kim, and M. E. Fisher, J. Phys. Chem. B **109**, 6824 (2005).

[24] E. Luijten, M. E. Fisher, and A. Z. Panagiotopoulos, Phys. Rev. Lett. **88**, 185701 (2002).

[25] Y. C. Kim, M. E. Fisher, and E. Luijten, Phys. Rev. Lett. **91**, 065701 (2003).

[26] A. M. Ferrenberg and R. H. Swendsen, Phys. Rev. Lett. **63**, 1195 (1989).

[27] M. E. Fisher and Y. Levin, Phys. Rev. Lett. **71**, 3826 (1993); Y. Levin and M. E. Fisher, Physica A **225**, 164 (1996).

[28] M. E. Fisher, J.-N. Aqua, and S. Banerjee, Phys. Rev. Lett. **95**, 135701 (2005); J.-N. Aqua, S. Banerjee, and M. E. Fisher, Phys. Rev. E **72**, 041501 (2005).